 doi:10.20944/preprints201804.0155.v1

Direct Exfoliation of g-C_3N_4 with Addition of NaOH for Enhanced Photocatalytic Cr(Ⅵ) Reduction

Yaping Guo[a], Jianyang Sun[a, b], Hui Chang[a], Xu Zhao[b, *]

[a] Zhejiang University of Technology, College of Environment, Hangzhou 310014, P. R. China

[b] Key Laboratory of Drinking Water Science and Technology, Research Center for Eco-Environmental Sciences, Chinese Academy of Sciences, Beijing 100085, China

Email: zhaoxu@rcees.ac.cn, luckyyaping@zjut.edu.cn

Tel: +86-10-62849667; Fax: +86-10-62849667

Preprints (www.preprints.org) | NOT PEER-REVIEWED | Posted: 11 April 2018 doi:10.20944/preprints201804.0155.v1

Table of contents

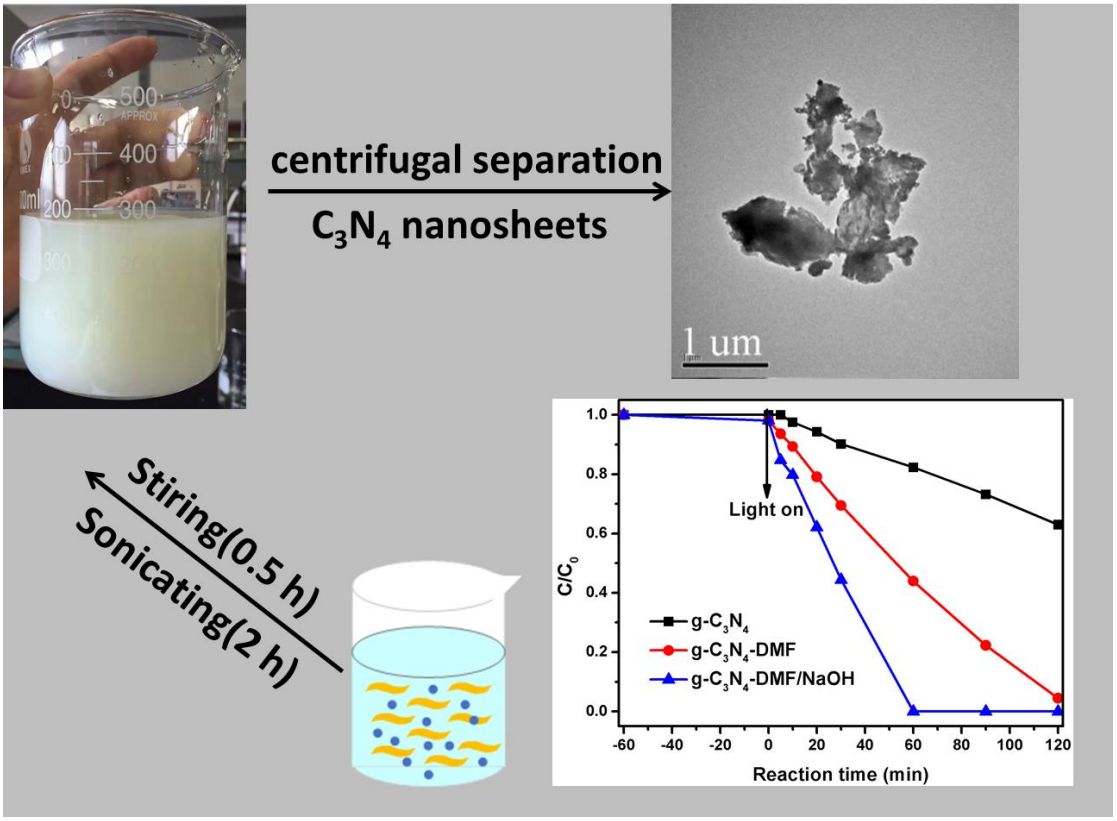

 doi:10.20944/preprints201804.0155.v1

Abstract

A simple, effective and environmental-friendly method was adopted for enhancing the photocatalytic activity of g-C_3N_4 in the reduction of aqueous Cr(Ⅵ) under visible-light irradiation. The enhancement was achieved via treatment of g-C_3N_4 in organic solvent with addition of NaOH particles by ultrasonic process for two hours. The results demonstrated that the treated g-C_3N_4 exhibited much higher photocatalytic activity than pristine g-C_3N_4 in the reduction of Cr(VI) . Under visible light irradiation for 120 min, the reduced ratios of Cr(VI) with the initial concentration of 50 mg/L in the presence of the treated g-$C_3N_4$and pristine g-C_3N_4 were 100% and 37.1%, respectively. With the addition of fulvic acid, Cr(VI) was efficiently removed at 40 min. Based on the characterization results of the structures and other physiochemical properties of the treated g-C_3N_4 and pristine g-C_3N_4 by X-ray diffraction, scanning electron microscopy, transmission electron microscopy and UV Vis diffuse reflectance, the possible reasons responsible for the enhanced photocatalytic activity of the treated g-C_3N_4 were proposed. The yield and mechanism of different exfoliation methods were compared by semi-quantitative method.

Key words: g-C_3N_4; photocatalysis; NaOH; exfoliation; Cr(VI) reduction

Preprints (www.preprints.org) | NOT PEER-REVIEWED | Posted: 11 April 2018 doi:10.20944/preprints201804.0155.v1

1. Introduction

Graphite-like Carbon nitride (g-C_3N_4) is a metal-free polymer with a band gap of about 2.7 eV. It is nontoxic, stable, and easy synthesized from rich and cheap CN-containing precursor [1]. In addition, it has been proved to have photocatalytic activity responsive to visible light in many chemical reactions [2-7]. Thus, g-C_3N_4 is regarded as a kind of promising photocatalyst for water splitting and degradation of organic pollutants under sunlight irradiation. Bulk g-C_3N_4 synthesized by the traditional thermal condensation polymerization shows low photocatalytic activity for its large particle size, small surface area and high recombination rate of photogenerated carriers[8]. So it is necessary to explore an effective and environmentally friendly method for improving the photocatalytic activies.

Bulk g-C_3N_4 has a layered structure with properties similar to that of graphite in which the C-C bond is replaced by a strong covalent C-N bond, and the layer is connected by a weak van der Waals force. g-C_3N_4 can be easily peeled off into monolayer or layers of nanosheets due to its graphite-like structure. It's reasonable that monolayered g-C_3N_4 nanosheets have excellent photocatalytic properties. For example, Wang firstly stirred it with strong acid (37% HCl) for 3 hours, reporting a reversible protonation of carbon nitride [7]; Liu and his colleagues developed a heat treatment to reduce its size [9]. From these results, the treated C_3N_4 showed much higher photocatalytic activities than the bulk g-C_3N_4 under visible light irradiation.

Preprints (www.preprints.org) | NOT PEER-REVIEWED | Posted: 11 April 2018 doi:10.20944/preprints201804.0155.v1

Notably, this method still has some disadvantages, such as the formation of the interface defects during the calcination process, the reduction of the photo absorption ability, the relatively thick nanosheet, and the poor yield (< 6%). These disadvantages for the photocatalytic reaction are critical. Although the exfoliation of high quality C_3N_4 2D nanosheets with low defects could also be achieved mechanically on a small scale, a simple liquid exfoliation method would allow the formation of 2D nanosheets in large quantities. Inspired by the graphene stripping method, some researchers have developed some liquid stripping methods to fabricate few-layered C_3N_4 nanosheets [10,11]. Unfortunately, the concentration of the as-prepared C_3N_4 nanosheets suspension is very low(anosheets su [11], and the monolayered nanosheet is limited [10], and the atomic structure of the plane during stripping maybe also seriously damage. Therefore, it's desired to develop a novel, facile, and rapid route to fabricate the C_3N_4 nanosheets.

In order to develop a simple, environmentally friendly and high-yield stripping method, NaOH were added into the organic solvent for liquid exfoliation of bulk g-C_3N_4 to produce monolayered C_3N_4 nanosheets for the first time, which improved the original liquid exfoliation process. On the basis of this, The photocatalytic activities of the untreated C_3N_4 and C_3N_4 nanosheets were compared by the reduction of Cr(Ⅵ) under visible-light (ed ies of liation tion of bulk g-C, 14</Yeardifferent organic acid. Moreover, the possible reasons responsible for the enhanced photocatalytic activity of the treated g-C_3N_4 were proposed based on the characterization results of the structures and other physiochemical properties of

Preprints (www.preprints.org) | NOT PEER-REVIEWED | Posted: 11 April 2018 doi:10.20944/preprints201804.0155.v1

untreated C_3N_4 and C_3N_4 nanosheets.

2. Experiment Section

2.1 Preparation of g-C_3N_4 nanosheets

The bulk g-C_3N_4 was prepared by polymorization of melamine molecules in a muffle furnace, melamine was heated at 600℃ for 4 h under air condition with a ramp rate of about 2.3℃/min in detail. The ultrathin g-C_3N_4 nanosheets were obtained by liquid exfoliating of as-prepared bulk g-C_3N_4 in organic solvent (DMF). In detail, 300 mg of untreated C_3N_4 was added into 250 ml of DMF and 50 mg of sodium hydroxide (NaOH) was added, and then sonicated for 2 h after magnetic stirring, the resulting solution was centrifuged and the supernatant was dried in air at a constant temperature, referred to as g-C_3N_4-DMF/NaOH. g-C_3N_4-DMF was obtained without the addition of NaOH for comparison.

2.2 Characterization of g-C_3N_4 nanosheets

The microstructure of g-C_3N_4 was characterized by field emission scanning electron microscopy (SEM, SU-8020, Hitachi, Japan) and transmission electron microscopy (TEM, H-7500, Hitachi, Japan). The crystal structure and functional groups were X-ray diffraction (XRD, X'Pert PRO MPD, Netherlands Panako Analytical Instruments Co., Ltd.) and UV-Vis diffuse reflectance spectroscopy (UV-VIS, Nicolet 8700, Thermo Fisher Scientific).

Photocatalytic activities of the samples (60 mg) were tested by the reduction of Cr(Ⅵ) with the initial concentration of 100 mg/L $K_2Cr_2O_7$ aqueous solution under

Preprints (www.preprints.org) | NOT PEER-REVIEWED | Posted: 11 April 2018 doi:10.20944/preprints201804.0155.v1

visible-light (ueous solu irradiation, with the addition of 1.0 mL of 100 mg/mL organic acid solution (citric acid, fulvic acid, oxalic acid) as sacrificing reagent. The concentration of Cr(Ⅵ) was measured by using diphenyl carbazide spectrophotometry(GB 7467-87).

3. Results and Discussion

3.1 Characterization of physiochemical properties of g-C_3N_4 nanosheets

Fig. 1 and 2 showed the SEM images of g-C_3N_4 obtained from different methods at different magnification. g-C_3N_4-DMF/NaOH sample still maintained loose and irregular tissue-like 2D nanosheet morphology at different magnification (Fig. 1c, Fig. 2), although a small portion of C_3N_4 nanosheets was stacked. Its morphology was quite different from that of the untreated g-C_3N_4 with a typical layer structure stacked layer by layer (Fig. 1a), g-C_3N_4-DMF had a thicker layered structure and more layers was stacked without the addition of NaOH.

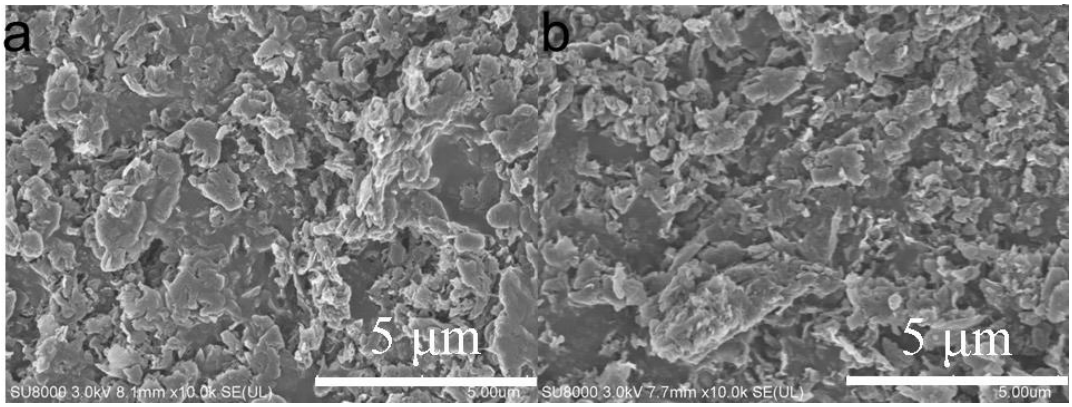

Preprints (www.preprints.org) | NOT PEER-REVIEWED | Posted: 11 April 2018 doi:10.20944/preprints201804.0155.v1

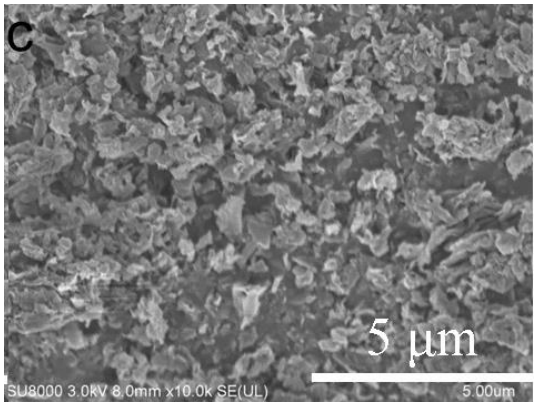

Fig. 1 SEM image of (a) g-C_3N_4 (b) g-C_3N_4-DMF; (c) g-C_3N_4-DMF/NaOH.

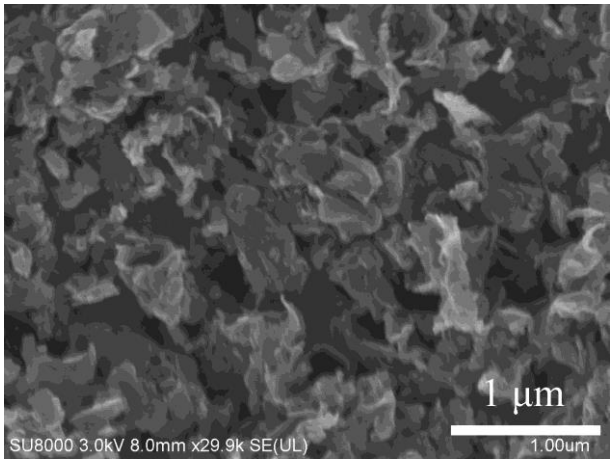

Fig. 2 SEM image of g-C_3N_4-DMF/NaOH-1 μm.

Fig. 3 showed the TEM images of g-C_3N_4-DMF/NaOH and g-C_3N_4-DMF. At different magnifications (1 μm, 0.5 μm and 0.2 μm), TEM images show that the as-prepared C_3N_4 (g-C_3N_4-DMF/NaOH) with laminar morphology exhibited nearly transparent feature, indicating its ultrathin thickness. Its lateral scale ranged from sub-micrometer to several micrometers. The horizontal scale range was about 3-4 μm. There are no obvious layered structure and obvious shadows observed at g-C_3N_4-DMF (Fig.3d, e, f). Smaller particle sizes mean that their photogenerated electrons and holes move from the site to the solid-liquid interface at a shorter distance, thereby reducing the recombination probability of their photogenerated carriers. [12,13]

Preprints (www.preprints.org) | NOT PEER-REVIEWED | Posted: 11 April 2018 doi:10.20944/preprints201804.0155.v1

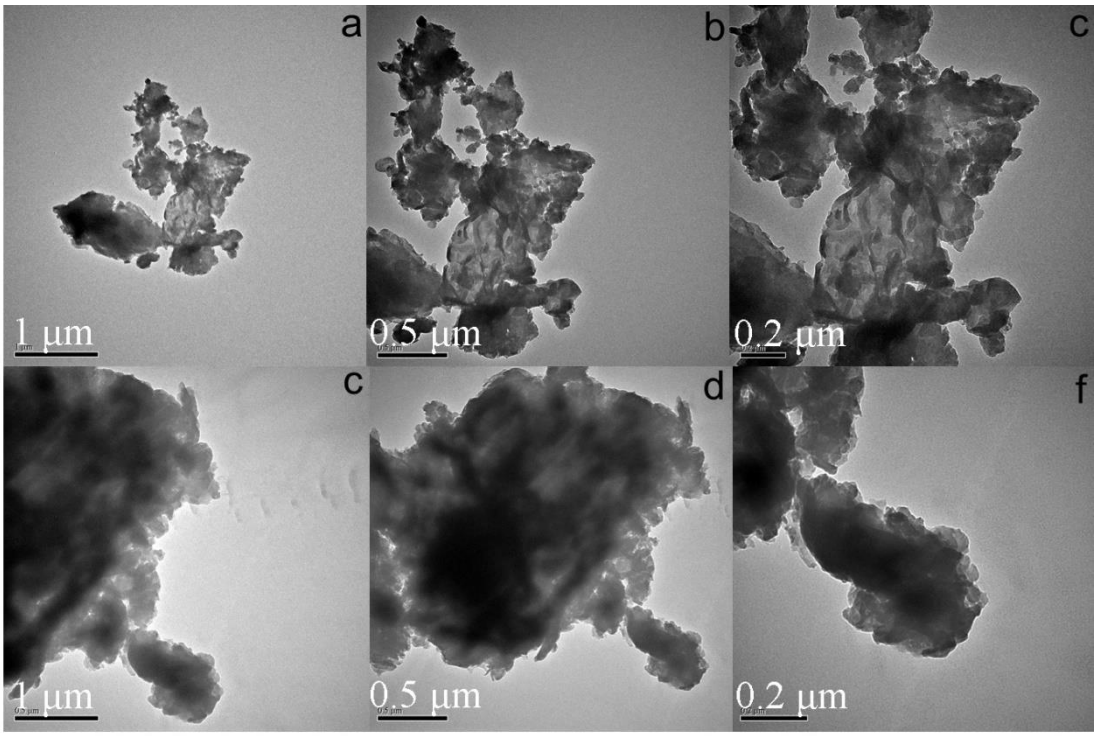

Fig. 3 TEM image of (a) g-C_3N_4-DMF/NaOH-1 μm; (b) g-C_3N_4-DMF/NaOH-0.5 μm; (c) g-C_3N_4-DMF/NaOH-0.2 μm; (d) g-C_3N_4-DMF -1 μm; (e) g-C_3N_4-DMF -0.5 μm; (f) g-C_3N_4-DMF -0.2 μm.

The ultra-thin thickness of g-C_3N_4-DMF/NaOH was further verified by the AFM image. As shown in Fig. 4, the representative AFM image shows a uniform thickness of about 0.38 nm. This thickness agrees well with the theoretical values of single-layer carbon nitride (0.324 nm) [14,15]. This can be used as a strong evidence for the presence of g-C_3N_4 nanosheets in the presence of monatomic layers in mixed solvents.

Preprints (www.preprints.org) | NOT PEER-REVIEWED | Posted: 11 April 2018 doi:10.20944/preprints201804.0155.v1

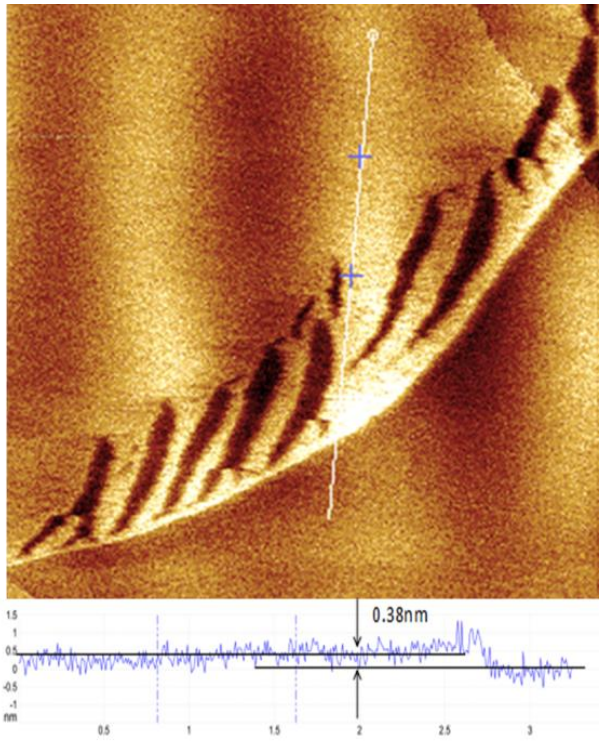

Fig. 4 AFM image of g-C_3N_4-DMF/NaOH.

Fig. 5 showed the XRD patterns of g-C_3N_4 nanosheets. It can be seen from the figure that the g-C_3N_4 nanosheet exhibits two distinct diffraction peaks at 13.2 ° and 27.3 °. The diffraction peak at 13.2 ° corresponds to the (100) crystal plane of g-C_3N_4 with the interplanar spacing of 0.676 nm, the 3-s-triazine ring structure of g-C_3N_4; the diffraction peak at 27.3 ° corresponds to g (002) crystal plane with the interplanar spacing of 0.324 nm, which is the accumulation of g-C_3N_4 aromatic structure, corresponding to the layer spacing of g-C_3N_4 [16]. As shown in the figure, the peak height of the diffraction peak at 27.3 ° decreases gradually from bottom to top, indicating that the intergranular stacking structure of g-C_3N_4 and the periodic arrangement of the layers are destroyed, indicating that g-C_3N_4 of is successfully stripped [12].

Preprints (www.preprints.org) | NOT PEER-REVIEWED | Posted: 11 April 2018 doi:10.20944/preprints201804.0155.v1

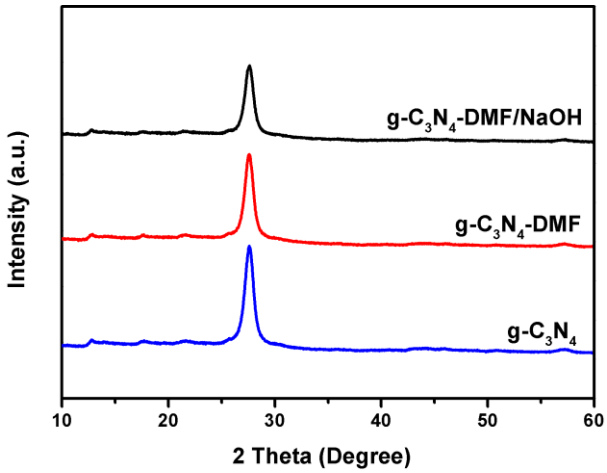

Fig. 5 XRD results of the g-C_3N_4 samples.

Fig. 6a showed the UV-Vis diffuse spectrum of g-C_3N_4. A typical semiconductor absorption, photogenerated electronstransfers from the valence band (VB) level formed by the N 2p orbit to the conduction band (CB) level formed by the C 2p orbit under irradiation, the absorption of as-prepared C_3N_4 in the visible region is significantly improved and exhibits a significant absorption boundary displacement. The absorption thresholds λg of g-C_3N_4, g-C_3N_4-DMF and g-C_3N_4-DMF/NaOH were 461, 472 and 494 nm, respectively. Using the formula [αhv]^n = A(hv - Eg) to calculate the band gap width Eg of g-C_3N_4, g-C_3N_4-DMF and g-C_3N_4-DMF/NaOH, where α is the absorption coefficient; hv is the photon energy and is a constant; Eg is the required band gap Width (optical bandgap); n is determined by the basic properties of the semiconductor (n = 2) [16,17]. The results are shown in Fig 6b, which are 2.53, 2.51, 2.44 eV, respectively. The results show that the addition of NaOH can change the band structure of g-C_3N_4, reduce the bandgap energy and improve the utilization rate of visible light.

Preprints (www.preprints.org) | NOT PEER-REVIEWED | Posted: 11 April 2018 doi:10.20944/preprints201804.0155.v1

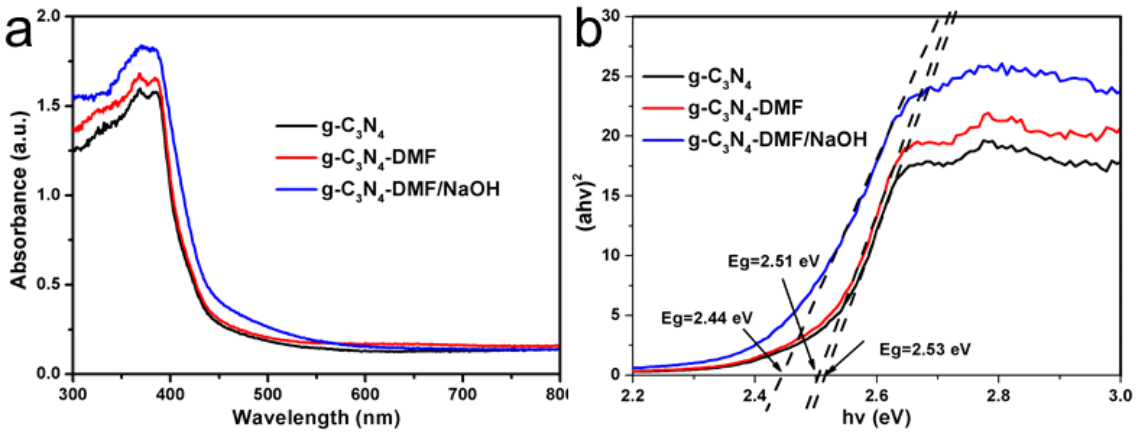

Fig. 6 UV-vis DRS spectra of g-C_3N_4.

3.2 Photocatalytic reduction of Cr(Ⅵ) by g-C_3N_4

As shown in Fig.7a, the removal efficiency of Cr(Ⅵ) is 37.1%, 95.5%, 100%, respectively, and the sequence of photocatalytic reduction activity is g-C_3N_4-DMF/NaOH > g-C_3N_4-DMF> g-C_3N_4; Cr(Ⅵ) can be completely removed in 60 min with g-C_3N_4-DMF/NaOH. g-C_3N_4 treated with NaOH shows the highest photocatalytic activity. In the initial 60 min string in dark, there is no change in the morphology of C_3N_4 after stripping, and the removal rate (adsorption) of Cr(Ⅵ) is almost ignored. Fig.7b shows the removal rate of Cr(Ⅵ) by photocatalytic reduction using the g-C_3N_4-DMF/NaOH samples with different organic acids as sacrificing reagent. The removal rate of Cr(Ⅵ) is almost ignored with organic acids (citric acid, fulvic acid, oxalic acid) alone. After the addition of the treated g-C_3N_4 nanosheets, Cr(Ⅵ) could be completely removed within 120 min (60 min, 40 min, 120 min, respectively)). The removal rate is related to the ability of different organic acids to capture the hole. The experimental results show that g-C_3N_4-DMF/NaOH samples can effectively remove Cr(Ⅵ) with different organic acids.

Preprints (www.preprints.org) | NOT PEER-REVIEWED | Posted: 11 April 2018 doi:10.20944/preprints201804.0155.v1

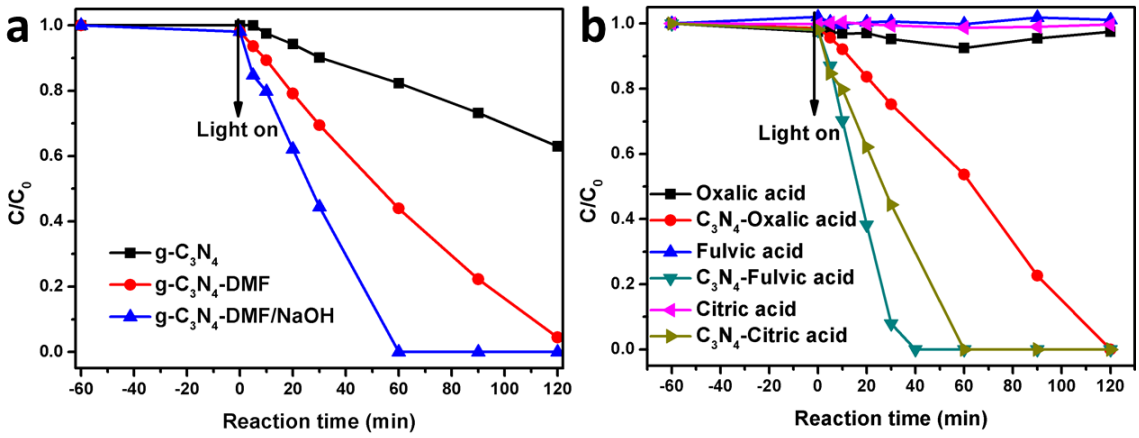

Fig. 7 (a) the photocatalytic reduction of Cr(VI) using different samples; (b) the effect of organic acids on the photocatalytic reduction of Cr(VI); Cr(VI initial concentration: 50 mg/L; organic acid concentration: 1 mg/L; 300 mW Xe lamp; l > 400 nm).

3.3 g-C_3N_4 nanosheet production and exfoliation mechanism

Fig. 8 shows the g-C_3N_4 nanosheet suspension (3000 rpm low-speed centrifuged supernatant) with different exfoliation methods. For the convenience of description, the products obtained in DMF or IPA were recorded as g-C_3N_4-DMF, g-C_3N_4-IPA and so on. As shown in the right-hand centrifuge tube of Figure 8a, the g-C_3N_4 nanosheets were dispersed to a maximum concentration, showing milky white (about 1.2 mg/ml). In contrast, pure DMF stripping showed a relatively low concentration (Figure 8a, left), showing a pale white (about 0.3 mg/ml). The experimental results showed that the addition of NaOH increased the yield of g-C_3N_4 nanosheets. This phenomenon verifies a fact that dispersed concentration is maximized when the energy of exfoliation is minimized. The energy of the exfoliation can be expressed by the enthalpy of mixing (ΔH_{mix}, unit volume), calculated from the empirical formula shown below (Eq 1) [18,19]:

Preprints (www.preprints.org) | NOT PEER-REVIEWED | Posted: 11 April 2018 doi:10.20944/preprints201804.0155.v1

$$\frac{\Delta H_{mix}}{V_{mix}} \approx \frac{2}{T_{nanosheet}} (\delta_{nanosheet} - \delta_{solvent})^2 \phi \qquad \text{Eq 1}$$

Where V is the volume of the suspension, δ is the square root of the surface energy, T is the average thickness of the nanosheets, and φ is the volume fraction of the nanosheets. The Hildebrand-Scratchard formula indicates that the enthalpy of mixing is dependent on the surface energy balance of C_3N_4 and solvent. For C_3N_4, the surface energy can be defined as the energy per unit area to overcome the energy required for the van der Waals force to separate the two pieces.

From the formula, we hope that the surface energy (δ_solvent) of the solvent matches the surface energy of the carbon nitride (δ_nanosheet) and obtain more nanosheets at the minimum energy cost. For a mixed system, the surface energy can be adjusted by simply changing their composition. In this case, NaOH is not soluble in DMF, but it effectively changes its surface energy, thereby increasing the yield of g-C_3N_4 nanosheets, which is consistent with the literature [20].

As shown in Figure 8a, b, c, we also studied the effect of NaOH on the yield of g-C_3N_4 nanosheets for several other organic solvents. The centrifugal tubes on the left side of each panel were centrifuged at 3000 rpm without adding NaOH, the right side of the supernatant is the one with the addition of NaOH. From the figure it is clearly seen the left side of the clarity in the clear, the right side of the milky white. After the collection, it was found that the addition of NaOH in different organic solvents for g-C_3N_4 nanosheet stripping could increase the yield, which was consistent with the results of the addition of NaOH in the organic solvent to increase the yield of

Preprints (www.preprints.org) | NOT PEER-REVIEWED | Posted: 11 April 2018 doi:10.20944/preprints201804.0155.v1

graphene nanosheets[20].

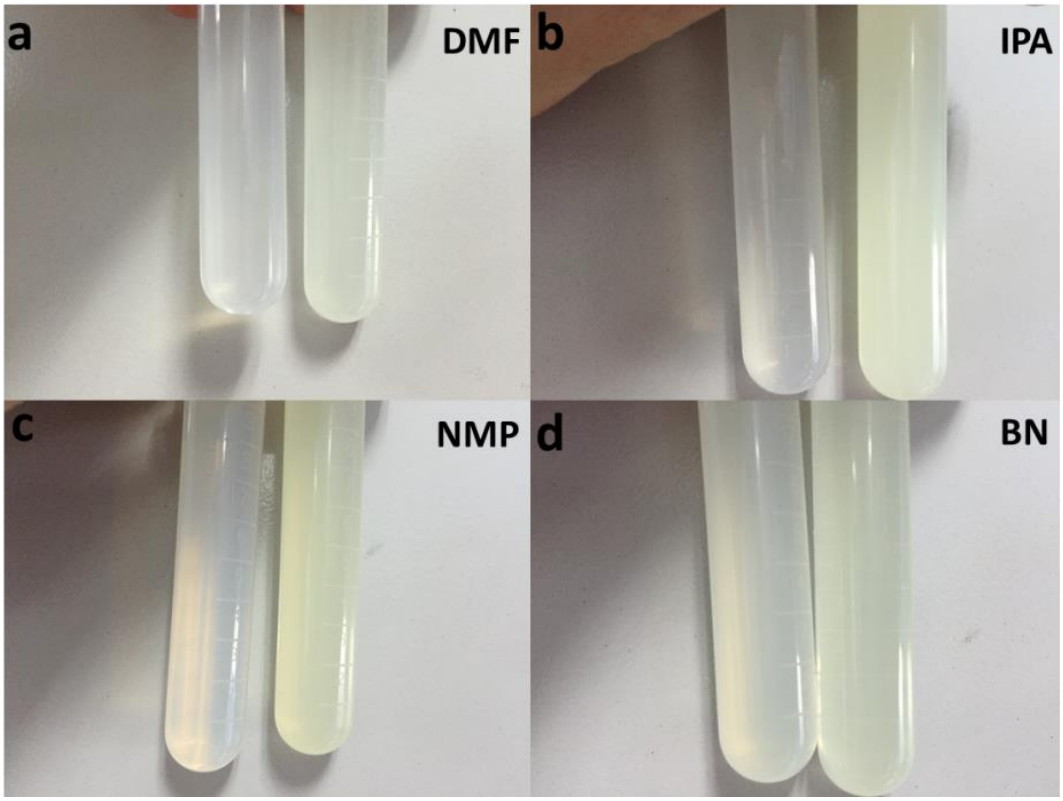

Fig. 8 C_3N_4 sheets dispersed in organic solvents with or without addition of NaOH.

4. Conclusions

In conclusion, monolayer C_3N_4 nanosheets have been successfully prepared by a new, simple solvent intercalation method. The poor solvent could be changed into good solvent by adding NaOH particles for efficiently exfoliating bulk g-C_3N_4 into C_3N_4 nanosheets. Importantly, the concentration of C_3N_4 nanosheets could be increased for 4 times by simply adding NaOH particles into the solvent. The as-prepared C_3N_4 nanosheets with monolayer thickness would be endowed a new band structure and superior photocatalytic properties, such as favorable band structure, higher visible light absorption efficiency, lower photo-generated electron-hole pair recombination efficiency, higher specific surface area, and low surface defects. More

 doi:10.20944/preprints201804.0155.v1

intuitive to say, the high degradation efficiency of Cr(Ⅵ) was obtained by the as-prepared C_3N_4 nanosheets. The removal efficiency of Cr(Ⅵ) is twice as high as that of g-C_3N_4-DMF, which is 6 times for bulk g-C_3N_4. g-C_3N_4-DMF/NaOH can be directly added to the organic acid leaching Cr(Ⅵ) wastewater for photocatalytic reaction, Cr(Ⅵ) can be completely removed (120 min) under three different organic acid conditions.

Acknowledgements

The authors gratefully acknowledge financial support from National Natural Science Foundation of China (No. 21377148, 51222802), the Key Project of Science and Technology of Zhejiang Province (No. 2011C14023) and National Natural Science Foundation of China for Young Scholars (No. 51108416)

References

1. Zhu, J.; Xiao, P.; Li, H.; Carabineiro, S.A.C. Graphitic carbon nitride: Synthesis, properties, and applications in catalysis. *ACS Applied Materials & Interfaces* **2014**, *6*, 16449-16465.
2. Cui, Y.; Zhang, G.; Lin, Z.; Wang, X. Condensed and low-defected graphitic carbon nitride with enhanced photocatalytic hydrogen evolution under visible light irradiation. *Applied Catalysis B: Environmental* **2016**, *181*, 413-419.
3. Nie, H.; Ou, M.; Zhong, Q.; Zhang, S.; Yu, L. Efficient visible-light photocatalytic oxidation of gaseous no with graphitic carbon nitride (g–c3n4) activated by the alkaline hydrothermal treatment and mechanism analysis. *Journal of Hazardous Materials* **2015**, *300*, 598-606.
4. Qin, J.; Wang, S.; Ren, H.; Hou, Y.; Wang, X. Photocatalytic reduction of co2 by graphitic carbon nitride polymers derived from urea and barbituric acid. *Applied*

Catalysis B: Environmental **2015**, *179*, 1-8.

5. Sano, T.; Tsutsui, S.; Koike, K.; Hirakawa, T.; Teramoto, Y.; Negishi, N.; Takeuchi, K. Activation of graphitic carbon nitride (g-c3n4) by alkaline hydrothermal treatment for photocatalytic no oxidation in gas phase. *Journal of Materials Chemistry A* **2013**, *1*, 6489-6496.
6. Shen, B.; Hong, Z.; Chen, Y.; Lin, B.; Gao, B. Template-free synthesis of a novel porous g-c3n4 with 3d hierarchical structure for enhanced photocatalytic h2 evolution. *Materials Letters* **2014**, *118*, 208-211.
7. Zhang, Y.; Thomas, A.; Antonietti, M.; Wang, X. Activation of carbon nitride solids by protonation: Morphology changes, enhanced ionic conductivity, and photoconduction experiments. *Journal of the American Chemical Society* **2009**, *131*, 50-51.
8. Wei, H.; Zhang, Q.; Zhang, Y.; Yang, Z.; Zhu, A.; Dionysiou, D.D. Enhancement of the cr(vi) adsorption and photocatalytic reduction activity of g-c3n4 by hydrothermal treatment in hno3 aqueous solution. *Applied Catalysis A: General* **2016**, *521*, 9-18.
9. Niu, P.; Zhang, L.; Liu, G.; Cheng, H.-M. Graphene-like carbon nitride nanosheets for improved photocatalytic activities. *Advanced Functional Materials* **2012**, *22*, 4763-4770.
10. Zhao, H.; Yu, H.; Quan, X.; Chen, S.; Zhao, H.; Wang, H. Atomic single layer graphitic-c3n4: Fabrication and its high photocatalytic performance under visible light irradiation. *Rsc Advances* **2014**, *4*, 624-628.
11. Zhang, X.; Xie, X.; Wang, H.; Zhang, J.; Pan, B.; Xie, Y. Enhanced photoresponsive ultrathin graphitic-phase c3n4 nanosheets for bioimaging. *Journal of the American Chemical Society* **2013**, *135*, 18-21.
12. Xu, J.; Zhang, L.; Shi, R.; Zhu, Y. Chemical exfoliation of graphitic carbon nitride for efficient heterogeneous photocatalysis. *Journal of Materials Chemistry A* **2013**, *1*, 14766-14772.
13. Xu, J.; Wang, Y.; Zhu, Y. Nanoporous graphitic carbon nitride with enhanced photocatalytic performance. *Langmuir* **2013**, *29*, 10566-10572.

14. Su, D.S.; Zhang, J.; Frank, B.; Thomas, A.; Wang, X.; Paraknowitsch, J.; Schloegl, R. Metal-free heterogeneous catalysis for sustainable chemistry. *Chemsuschem* **2010**, *3*, 169-180.
15. Wang, Y.; Wang, X.; Antonietti, M. Polymeric graphitic carbon nitride as a heterogeneous organocatalyst: From photochemistry to multipurpose catalysis to sustainable chemistry. *Angewandte Chemie-International Edition* **2012**, *51*, 68-89.
16. Ran, J.; Ma, T.Y.; Gao, G.; Du, X.-W.; Qiao, S.Z. Porous p-doped graphitic carbon nitride nanosheets for synergistically enhanced visible-light photocatalytic h-2 production. *Energy & Environmental Science* **2015**, *8*, 3708-3717.
17. Di, J.; Xia, J.; Li, X.; Ji, M.; Xu, H.; Chen, Z.; Li, H. Constructing confined surface carbon defects in ultrathin graphitic carbon nitride for photocatalytic free radical manipulation. *Carbon* **2016**, *107*, 1-10.
18. Hernandez, Y.; Nicolosi, V.; Lotya, M.; Blighe, F.M.; Sun, Z.; De, S.; McGovern, I.T.; Holland, B.; Byrne, M.; Gun'ko, Y.K., *et al.* High-yield production of graphene by liquid-phase exfoliation of graphite. *Nature Nanotechnology* **2008**, *3*, 563-568.
19. Coleman, J.N.; Lotya, M.; O'Neill, A.; Bergin, S.D.; King, P.J.; Khan, U.; Young, K.; Gaucher, A.; De, S.; Smith, R.J., *et al.* Two-dimensional nanosheets produced by liquid exfoliation of layered materials. *Science* **2011**, *331*, 568-571.
20. Liu, W.W.; Wang, J.N. Direct exfoliation of graphene in organic solvents with addition of naoh. *Chemical Communications* **2011**, *47*, 6888-6890.